Chapter 5

Models

5.1 Tennant

Tennant developed a universal rule-of-thumb method, that is designed to be applied to streams of all sizes and to work independantly of the fish and other species. It is based on dividing the year into two seasons and defining flow regimes as a fraction of the average flow. Since the average flow knowingly varies strongly for the pre- and post-impact period, all calculations have been undertaken seperately in the respective pre- and post-time-series, in order to compare the results interpretability. Results can be seen in table 5.1.

	Pre-impact		Post-impact	
Description of flows	Oct.-Mar.	Apr.-Sep.	Oct.-Mar.	Apr.-Sep.
Flushing or maximum	1164,48	1164,48	638,30	638,30
Optimum range	349,34	465,79	191,49	255,32
Outstanding	232,89	349,34	127,66	191,49
Excellent	174,67	291,12	95,74	159,57
Good	116,44	232,89	63,83	127,66
Fair or degrading	58,22	174,67	31,91	95,74
Poor and minimum	58,22	58,22	31,91	31,91
Severe degradation	29,11	29,11	15,95	15,95

Table 5.1: *Results from Tennant method for pre- and post-impact data. Definitions were calculated as fractions of the average flow as follows: Flushing 200%, optimum 60% (winter) and 80% (summer), outstanding 40% (winter) and 60% (summer), excellent 30% (winter) and 50% (summer), good 20% (winter) and 40% (summer), fair 10% (winter) and 30% (summer), poor 10% and severe degradation 5%.*

5.1.1 Discussion

The Tennant method delivers quick results that may be used as a reference guide for initial planning purposes. The method obtains results for flushing flows as well as optimum instream flow regimes. Results indicate that instream flows for the post-impact period

should be allocated above 96 m^3/s between october and march and above 160 $^3/s$ for april to september. Flushing flows are estimated at approximately 640 ^{3}. Results determined via the Tennant method have to be compared to results obtained from subsequent methods if possible in any way.

5.2 Range of Variability

As part of the RVA methodology [11] suggest the usage of IHA (Indicators of Hydrological Alteration) in order to assess pre-impact post-impact changes. This is done by

1. Defining the data series e.g. Pre-/post-impact time frames
2. Calculate values of intra-annual hydrological attributes
3. Compute inter-annual statistics
4. Calculate values of the IHA

5.2.1 Parameters

The RVA analysis was applied to the data-set obtainable from the CHE for the Tortosa gauging station using the IHA software freely available from the Nature Conservancy website. Selected was a two-period setup, the pre-impact series reaching from 1913-1935 and the post-impact from 1975-2002. Hi- and low-pulse levels were defined with one standard deviation, likewise were the upper and lower RVA limit. All data gaps lacking more than 10 data-sets were told to be treated as missing.

Time-range	Start	End
Pre-dam time series	1st of january 1913	31st of october 1935
Post-dam time series	1st of november 1975	30th of september 2002

Table 5.2: *Time-range used for RVA analysis*

5.2.2 Error

As reported by the algorithm, there exists a data gap of 94 days in the original data-set. Data gaps are being interpolated as can be seen in the software documentation. Current interpolation algorithms undertake linear interpolation across year boundaries. If the adjacent year is missing, the last good date is duplicated to the year boundary. In years with very large gaps in the data, this can lead to odd results for rise/fall rates, pulses, and other parameters. Thus the graphical output has to be observed as well. Larger gaps can be observed for the years 1984/85. On the 22nd of october 1984 data is missing until the 22nd of january 1985. Later on during 1985 there occur some more data gaps starting from the 2nd of november ending on the 31st of december. In the year 1989 some smaller but more frequent data gaps occur. Since the data range would be

fairly small from 1977 until 1984 it was decided to include the data range containing frequent gaps. According to the log messages of the IHA software the 25^{th} percentile for the lower RVA limit is used instead of one standard deviation for

- Low pulse count
- Low pulse duration

For the upper limits corrections are undertaken replacing the boundary by the 75^{th} percentile for

- 1-day minimum
- 3-day minimum
- 7-day minimum
- 30-day minimum

Reviewing the above IHA attributes, the graphical output delivers a broad jump for the 1-day minimum from 1924-1929. 3-day minimum shows a harsh decline between 1926-1929 similar to the 7-day and 30-day minimum flow. Hence they were omitted. Analogous to the above attributes, the 90-day minimum shows a decrease in the same period, though the decline is not as harsh as. Thus the 90-day minimum might be considered for further analysis. The low pulse count attribute delivers data from 1925 only, thus low pulse count and low pulse duration are being omitted.

5.2.3 IHA Results

Results calculated comprise mean, coefficient of dispersion and their respective deviations as mentioned before. In order to determine the quality of the results, the graphical output in conjunction with the coefficient of dispersion is being analyzed. Graphical output helps determining outliers or similar errors. In combination with the coefficient of dispersion this draws a picture of reasonability of IHA parameters calculated. Thus certain IHA attributes can be selected, that may be interpreted using results from RVA calculations.

Table 5.3: IHA scorecard for Tortosa discharge data

	Mean		C.V.		Δ Mean		Δ C.V.	
	Pre	Post	Pre	Post	Magnitude	%	Magnitude	%
90-day min.	197,4	131,8	0,37	0,4	-65,6	-33	0,04	9,9
1-day max.	2844	1569	0,26	0,52	-1274,9	-45	0,26	101
3-day max.	2492	1443	0,3	0,51	-1049	-42	0,21	71,3
7-day max.	2036	1263	0,38	0,52	-773,3	-38	0,14	37,5
30-day max.	1358	884,7	0,36	0,48	-473,5	-35	0,12	32,7

continued on next page

Table 5.3: IHA scorecard for Tortosa discharge data

	Mean		C.V.		Δ Mean		Δ C.V.	
	Pre	Post	Pre	Post	Magnitude	%	Magnitude	%
90-day max.	1003	659,3	0,34	0,4	-343,3	-34	0,06	18,6
High pulse No.	8,8	2,1	0,45	1,09	-6,7	-76	0,63	140
High pulse Δt	4,8	3,2	0,51	0,98	-1,6	-33	0,47	92,4
Rise rate	152,9	60,8	0,3	0,48	-92,1	-60	0,17	57,4
Fall rate	-82,6	-56,6	-0,31	-0,5	26,1	-32	-0,18	58,5
No. of reversals	108,8	171,9	0,21	0,09	63,1	58	-0,12	-58,2
October	332,5	209,1	0,59	0,65	-123,4	-37	0,06	9,7
November	573,3	328,5	0,46	0,61	-244,8	-43	0,14	30,8
December	731,5	375,1	0,46	0,69	-356,4	-49	0,23	49,9
January	667,5	507,9	0,34	0,59	-159,6	-24	0,25	72,6
February	763,1	573,9	0,49	0,78	-189,3	-25	0,29	60
March	950	416,6	0,49	0,64	-533,4	-56	0,15	30,9
April	815,4	399	0,48	0,64	-416,4	-51	0,16	33,4
May	851,6	381,6	0,49	0,58	-470,1	-55	0,09	18
June	671,9	325,8	0,5	0,87	-346,1	-52	0,37	74,8
July	325,9	174,7	0,58	0,61	-151,1	-46	0,02	4,1
August	174	129,2	0,4	0,43	-44,8	-26	0,03	6,9
September	214,8	156,1	0,36	0,42	-58,7	-27	0,05	14,9

Observing obtained results (see table 5.3), it is eminent that apart from the number of reversals all other IHA attributes have decreased relatively over time (see also figure 5.1). This goes along with an increase in the deviation of the C.V. The latter might be explained by the decreasing mean, since the mean is reciprocally included in the coefficient of variation.

5.2.4 RVA Results

In order to relate the pre- and post-impact time-series the term range of variability has been invented by [11]. In this example of its application the range boundaries are being defined as the mean +/- one standard deviation to divide into highest, middle and lowest range as defined in 4.2.1. Based on these results the hydrologic alteration is being calculated as explained beforehand. Since the IHA have already been verified, it is possible to directly quote the alteration factors for the upper, middle and lower categories.

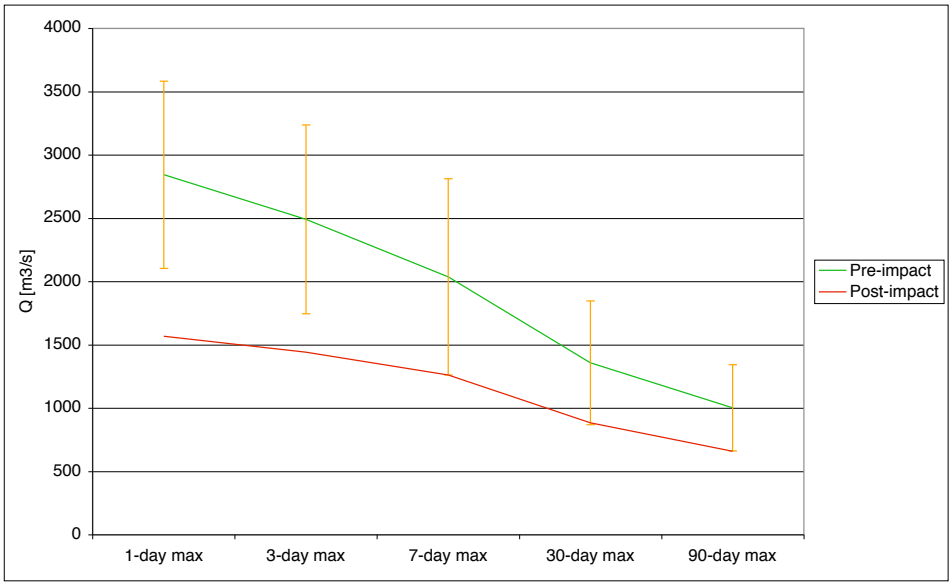

Figure 5.1: *Illustrated are pre-impact data for maximum IHA parameters including +/- one standard deviation as a measure of scatter. Post-impact data is located systematically below pre-impact data, outside one standard deviation for events with larger magnitude.*

Table 5.4: Results for RVA categories from Tortosa discharge data

	Middle RVA Category			Highest RVA Category			Lowest RVA Category		
	Exp.	Obs.	Alt.	Exp.	Obs.	Alt.	Exp.	Obs.	Alt.
October	17,18	15	-0,13	2,86	1	-0,65	0,95	5	4,24
November	15,27	8	-0,48	3,82	0	-1	1,91	13	5,81
December	13,36	6	-0,55	5,73	0	-1	1,91	15	6,86
January	17,18	10	-0,42	1,91	1	-0,48	1,91	10	4,24
February	12,41	11	-0,11	5,73	2	-0,65	2,86	8	1,79
March	16,23	7	-0,57	1,91	0	-1	2,86	14	3,89
April	12,41	6	-0,52	3,82	0	-1	4,77	15	2,14
May	16,23	6	-0,63	2,86	0	-1	1,91	15	6,86
June	17,18	5	-0,71	1,91	1	-0,48	1,91	15	6,86
July	15,27	10	-0,35	3,82	1	-0,74	1,91	10	4,24
August	14,32	11	-0,23	1,91	1	-0,48	4,77	9	0,89
September	12,41	11	-0,11	4,77	1	-0,79	3,82	9	1,36
90-day min.	12,41	7	-0,44	2,86	1	-0,65	5,73	13	1,27
1-day max.	14,32	5	-0,65	2,86	0	-1	3,82	16	3,19
3-day max.	15,27	6	-0,61	2,86	0	-1	2,86	15	4,24
7-day max.	16,23	10	-0,38	3,82	0	-1	0,95	11	10,52
30-day max.	17,18	10	-0,42	2,86	0	-1	0,95	11	10,52
90-day max.	17,18	9	-0,48	2,86	0	-1	0,95	12	11,57
High pulse No.	13,36	2	-0,85	4,77	0	-1	2,86	19	5,63
High pulse Δt	14,32	10	-0,3	2,86	2	-0,3	3,82	9	1,36
Rise rate	13,36	1	-0,93	4,77	0	-1	2,86	20	5,98
Fall rate	14,32	7	-0,51	2,86	13	3,54	3,82	1	-0,74
No. of reversals	13,36	0	-1	3,82	21	4,5	3,82	0	-1

What could be assumed in the IHA attribute analysis can be verified by RVA results as seen in table 5.4. Whereas the middle and the upper RVA category show a negative alteration, meaning that less frequently events occur above the mean minus one standard deviation, the lower RVA category accounts a positive alteration. Thus it can be concluded that the event distribution for the respective IHA parameters observed has changed in the way that events in the post-impact phase are more frequently scattered at lower levels than in the pre-impact distribution. Unfortunately the majority of the minimum flow events could not be consulted. From results concerning the 90-day minimum flow it may be suggested, that event distribution has not lowered but rather consolidated at the lower middle category end. Results for changes in mean and in the coefficient of dispersion (C.V.) can be seen in table 5.5.

Table 5.5: RVA scorecard for Tortosa discharge data

	Mean		C.V.		Δ Mean		Δ C.V.	
	Pre	Post	Pre	Post	Magnitude	%	Magnitude	%
90-day min.	197,4	131,8	0,37	0,4	-65,6	-33	0,04	9,9
1-day max.	2844	1569	0,26	0,52	-1274,9	-45	0,26	101
3-day max.	2492	1443	0,3	0,51	-1049	-42	0,21	71,3
7-day max.	2036	1263	0,38	0,52	-773,3	-38	0,14	37,5
30-day max.	1358	884,7	0,36	0,48	-473,5	-35	0,12	32,7
90-day max.	1003	659,3	0,34	0,4	-343,3	-34	0,06	18,6
High pulse No.	8,8	2,1	0,45	1,09	-6,7	-76	0,63	140
High pulse Δt	4,8	3,2	0,51	0,98	-1,6	-33	0,47	92,4
Rise rate	152,9	60,8	0,3	0,48	-92,1	-60	0,17	57,4
Fall rate	-82,6	-56,6	-0,31	-0,5	26,1	-32	-0,18	58,5
No. of reversals	108,8	171,9	0,21	0,09	63,1	58	-0,12	-58,2
October	332,5	209,1	0,59	0,65	-123,4	-37	0,06	9,7
November	573,3	328,5	0,46	0,61	-244,8	-43	0,14	30,8
December	731,5	375,1	0,46	0,69	-356,4	-49	0,23	49,9
January	667,5	507,9	0,34	0,59	-159,6	-24	0,25	72,6
February	763,1	573,9	0,49	0,78	-189,3	-25	0,29	60
March	950	416,6	0,49	0,64	-533,4	-56	0,15	30,9
April	815,4	399	0,48	0,64	-416,4	-51	0,16	33,4
May	851,6	381,6	0,49	0,58	-470,1	-55	0,09	18
June	671,9	325,8	0,5	0,87	-346,1	-52	0,37	74,8
July	325,9	174,7	0,58	0,61	-151,1	-46	0,02	4,1
August	174	129,2	0,4	0,43	-44,8	-26	0,03	6,9
September	214,8	156,1	0,36	0,42	-58,7	-27	0,05	14,9

Reviewing results for monthly RVA alteration it can be said generally, that the post-impact series has been flattened to the lower end of the pre-impact RVA middle boundary. Changes between high-flows for the pre-/post-impact series are greater than for low-flows during late summer. As has been proven in chapter 3.1.3 the extreme event distribution has changed due to the construction of dams and reservoirs and can be related to the reservoir capacity under certain circumstances. Interesting to observe is that the time range for the flood-period has shifted from march-may for the pre-impact series to january-march for the post-impact series (see also figure 5.2). This change is crucial, since this shift provides flood events under colder conditions, whereas the flora and fauna might need different hydraulic conditions at a later point throughout the year. This might have occurred due to reservoir regulation impact, reserving storage capacity to buffer the upstream flood period between march and may. Also this might occur due to changes in the run-off characteristics of the Ebro basin.

Detailed data for IHA parameters can be looked up in table B.1.

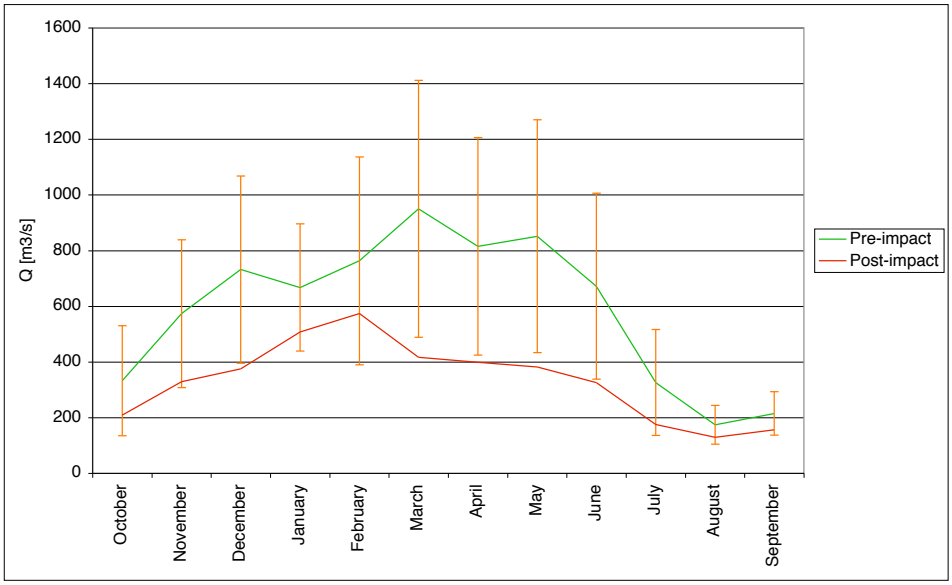

Figure 5.2: *IHA parameter: monthly values with pre-impact vs. post-impact. Illustrated is the pre-impact series with +/- one standard deviation. Note overlapping of IHA parameter boundaries defined by their standard deviations.*

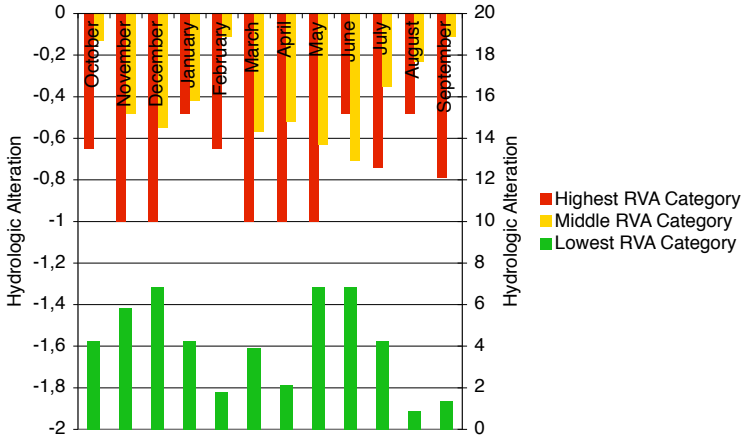

Figure 5.3: *Months: Hydrological alteration; Lowest category on 2nd axis. Frequency for illustrated IHA parameters drops for the highest and middle RVA category for the post-impact series. Observe more frequent occurence in the lowest RVA category. All hydrologic alterations fall below 33% and thus are very small.*

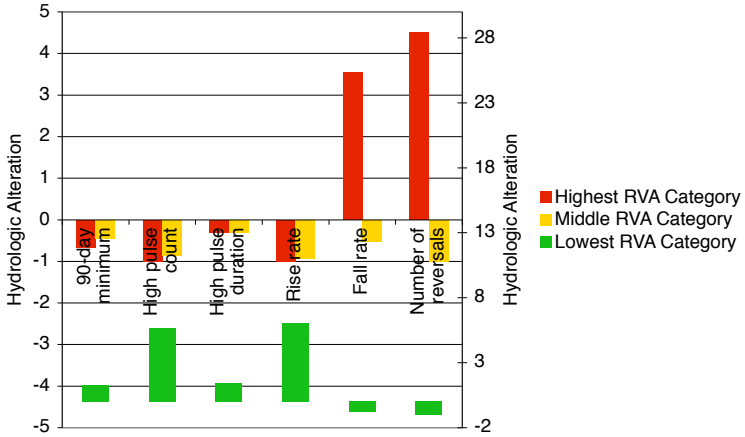

Figure 5.4: *Misc: Hydrological alteration; Lowest category on 2nd axis. Falling occurence for highest and middle RVA category for the first four parameters can be observed and an increasing frequency for the lowest RVA category. For the IHA parameter* $fall\ rate$ *and number* of $reversals$ *reciproque effects can be observed. All hydrologic alterations are very small.*

5.2.5 Discussion

Although most IHA parameters overlap respecting a +/- one standard deviation error, it is obvious for all monthly values and maximas, low and high pulses and all other parameters apart from the fall rate, that a harsh shift in mean has occurred. It is likely that these changes in flow regime have had its effects on the river ecology. However it is improbable that theoretical changes can all be proven in a reasonable time range, since ecological pre-impact data is rare and not much contemporary study on the river ecology has been undertaken neither. Further is not be reasonable to attempt a synthetic regulation of hydrologic dynamics as gathered from the pre-impact series, but a few attributes should be considered crucial for development for fluvial ecologic environment like nutrient exchange with flood plains.

- 90-day minimum: HA_{high}=-0,7; HA_{middle}=-0,4; HA_{low}=1,27; Although the minimum values should be considered with care due to changes in the observation instrumentation, it can be observed that in the higher and middle category occurrence is less after the increase in reservoir volume. Lower values can be observed though more frequently. This leads to the assumption that the duration of stressful chemical conditions has decreased.

- 1-day maximum: HA_{high}=-1; HA_{middle}=-0,7; HA_{low}=3,19; Decrease in occurrence in higher and middle category and increase in lower category. Thus the balance of competitive, ruderal and stress-tolerant organisms is changed. Due to a decrease in extremal events the competition is diminished.

- 3-day maximum: HA_{high}=-1; HA_{middle}=-0,6; HA_{low}=4,24; As seen in 1-day max

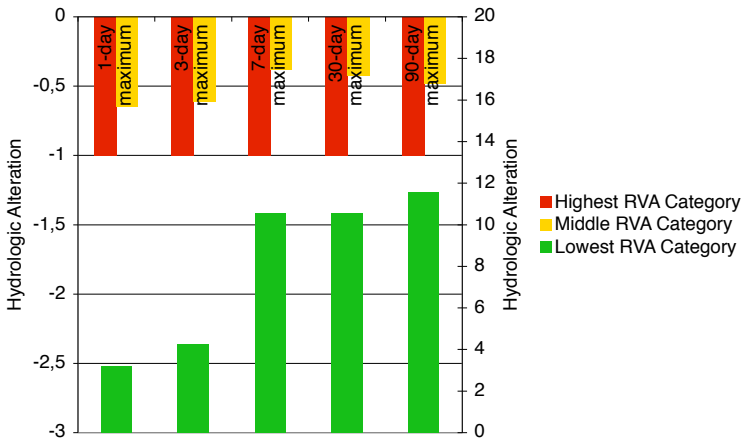

Figure 5.5: *Maximum: Hydrological alteration; Lowest category on 2nd axis. Observed frequencies for highest and middle RVA drop, whereas occurence in the lowest category rises. All hydrologic alterations are very small.*

although the increase in lower category is stronger. Hence it can be assumed than the structuring of the river channel morphology and physical habitat conditions has changed. Morphology changes can be observed from the comparison of historic aerial photos with current ones.

- 7-day maximum: HA_{high}=-1; HA_{middle}=-0,4; HA_{low}=10,5; As seen in 3-day max only the increase in lower category is even stronger. It can be assumed that dehydration in animals occurs, due to less frequent available water in flood plains.
- 30-day maximum: HA_{high}=-1; HA_{middle}=-0,4; HA_{low}=10,5; As seen in 7-day max only the increase in lower category is even more stronger. This way the nutrient volume exchange between flood plains and rivers is decreased, since less water body volume is in interference with flood plains.
- 90-day maximum: HA_{high}=-1; HA_{middle}=-0,5; HA_{low}=11,6; As seen in 30-day max with even stronger increase in lower category. It can be assumed that the stressful chemical conditions such as low oxygen and nutrient content in the aquatic environment have been decreased.
- Date of minimum: HA_{high}=0,68; HA_{middle}=-0,8; HA_{low}=4,24; Occurrence for above and below 1 std. deviation have increased for the post-impact series, whereas frequency of occurrence for the middle period has decreased. Thus it can be assumed that the Julian date for the 1-day minimum is more scattered throughout the time-series and thus the predictability of organism stress is less.
- Date of maximum: HA_{high}=-0,6; HA_{middle}=-0,4; HA_{low}=0,57; Occurrence for both middle and higher category has decreased for this IHA parameter. Hence the Julian date of the 1-day maximum occurs statistically earlier, as seen already with the monthly distribution. In that way reproduction cycles like spawning cues for migratory fish are changed or to avoid predation and hence a shift in species occurrence might occur.
- High pulse count: HA_{high}=-1; HA_{middle}=-0,9; HA_{low}=5,63; The high pulse count has shifted clearly to the lower RVA category. Thus the frequency and magnitude of soil moisture stress for plants is decreased and less water is available for plant consumption.
- High pulse duration: HA_{high}=-0,3; HA_{middle}=-0,3; HA_{low}=1,36; In parallel to the high pulse count the flood events are also shorter with an increasing HA for the lower category. Thus flood-plains habitats are less available for aquatic organisms and nutrient and organic matter exchange is decreased.
- Rise rate: HA_{high}=-1; HA_{middle}=-0,9; HA_{low}=5,98; As a measure for a rate of change the rise rate has decreased statistically for the post-impact time-series. Hence the draught stress on plants has increased due to the lower positive differences between consecutive daily values.
- Fall rate: HA_{high}=3,54; HA_{middle}=-0,5; HA_{low}=-0,7; In contrast to the rise rate, the fall rate has increased. This way the entrapment of organisms on islands and flood-plains becomes more likely.

- Number of reversals: HA_{high}=4,5; HA_{middle}=-1; HA_{low}=-1; The number of flow reversals has increased for the post-impact time-series. This way the desiccation stress on low-mobility stream edge organisms rises.

Although IHA parameters allow for detailed interpretation, hydrologic alterations calculated are very small. This is mostly due to the fact that +/- one standard deviation boundaries overlap for the pre- and post-impact series and thus cannot deliver larger values for its hydrologic alteration. It thus can be concluded the more disperse the IHA parameter input signal the larger the standard deviation and the smaller the hydrologic alterations, although changes in mean might be large. Hence the quality of the data basis becomes even more important. The RVA provides a very good tool in order to control future flow dynamics for its quality. Thus e.g. a 10 years discharge might be synthesized and applying the RVA the hydrologic alteration results serve as a direct quality measures for its dynamics. Future time-series should though always refer to the pre-impact phase, since it represents the former flow dynamics nature of the ecosystem.

5.2.6 Conclusion

Applying the RVA to the Tortosa discharge time-series the following consequences can be drawn

- The RVA allows for interpretation of flow dynamics in ecological terms.
- Most IHA parameters have changed their frequency of occurence from the highest and middle RVA category towards the lowest.
- The yearly flood peak of monthly discharge distribution has shifted in time from march-may to january-march and decreased in mean.
- Observed hydrologic alterations are very small, due to large standard deviation values, which define category boundaries and allow for overlapping.
- The RVA does not deliver numeric flow recommendations but provides a good flow dynamics quality control measure. Thus synthesized series may be analyzed before its application.

5.3 Phabsim

5.3.1 Data Basis

Simulations are being based on data given by Prof. Ernest Bladé of the hydraulics department of the UPC. It is available in HEC-RAS format with cross-sections between Flix, Xerta and Tortosa. Stage-Discharge graphs are available for each of the three sections mentioned.

5.3.2 Cross-Sections

Since all data is being compared to the gauging data-set at Tortosa gauging station, it was being considered reasonable to adapt the area of simulation accordingly. Thus the reach between Tortosa and Xerta is being selected for hydraulic simulation purposes as seen in table 5.6.

Original data-set		Tortosa-Xerta	
Section	Meter	Section	Meter
322 (Xerta)	54509,3	1	0
413 (Tortosa)	70069,2	91	15559,9

Table 5.6: *Selected area for backwater curve simulation. Distances are being defined from the river mouth for the original data-set and relatively to the downstream stage-discharge section for the modeling data-set.*

5.3.3 Hydraulic Simulation

Three water surface models are available within the Phabsim software package. The STGQ (Stage-Discharge) and the MANSQ (Manning's equation) treat cross-sections independently, whereas the WSP (Backwater surface calculation) combines cross-section simulation results. Both STGQ and MANSQ though fairly easy to calibrate do not perform well for larger discharges, so for simulations the WSP is being selected.

The WSP backwater curve simulation program is based on the approach that the energy flux into a control volume minus the energy flux out of the control volume plus the time rate of energy change within the control volum equals zero. Using the Bernoulli energy equation the energy balance can be written as follows

$$[\frac{p_1}{\gamma} + \frac{v_1^2}{2g} + z_1] - [\frac{p_2}{\gamma} + \frac{v_2^2}{2g} + z_2] + [H_L] = 0 \tag{5.1}$$

Whereas p signifies pressure, γ the specific weight, v velocity, z the geodetic height and H_L the head loss. Subindexes mark upstream (2) and downstream (1) section. Thus the head loss can be calculated as the difference in energy between upstream and downstream section. In turn head loss defines energy slope gradient in the form of

$$S_1 = \frac{H_L}{L} \tag{5.2}$$

Whereas L defines the length of the reach in focus. Also the energy slope can be defined via the Mannings equation in the following way

$$S_2 = \frac{n^2 Q^2}{R^{4/3} A^2} \tag{5.3}$$

With Q as discharge, R as wetted perimeter, A the cross-section area and n as the Manning coefficient. This way two cross-sections can be related using the energy balance and energy slope definitions, so that with a known Manning coefficient

other values, e.g. stage can be calculated. For subcritical flow calculations can be undertaken upstream. Thus applying this technique to the Ebro reach, stage-discharge observations downstream are extrapolated upstreamwards.

It is known that for rising discharge values the Manning coefficient decreases and in revers and thus the Manning coefficient is a function of discharge. In order to implement this relation in the WSP model, a roughness modifier value is being introduced, which follows the relation

$$RMOD = a * Q^b \tag{5.4}$$

Whereas a and b resemble fitting coefficients. Hence the roughness modifier functions as a multiplier for the Manning coefficient, which can be theoretically fitted to the above function.

First of all though the data files have to be prepared. Therefore HEC-RAS is being converted to a HEC-2 compatible format using a fortran program from Prof. Ernest Bladé. Also cross-section distances have to be entered manually, due to import filter difficulties. Firstly for all sections the WSP simulation model is being assigned. Secondly the boundary condition is defined at the most downstream section. Phabsim takes nine stage-discharge samples that are entered for every discharge simulated. In order to do so the simulated discharges are defined as seen in table 5.7. Values applied for the Tortosa cross-section have been observed in the field. Upstream stage-discharge calibration data has been taken from [20].

Tortosa		Xerta	
Q [m^3/s]	H [m]	Q [m^3/s]	H [m]
400	1,62	400	5,46
700	2,51	700	6,45
1000	3,32	1000	7,3
2000	5,73	2000	9,66
3000	7,88	3000	11,66
4000	9,88	4000	13,46

Table 5.7: *Stage-discharge observations (Xerta) and extrapolations (Tortosa)*

5.3.4 Calibration

In order to calibrate the hydraulic step backwater curve model the following steps are undertaken

1. Extrapolation of observed downstream discharges in order to coincide with upstream observations.
2. Calibration of Manning coefficient using reference discharge of Q=1000 m^3/s.
3. Calibration of roughness modifications due to discharge variations.

In order to calibrate the hydraulics step-backwater model the stage-discharge measurements for Tortosa respectively Xerta are used. Since the measurements at Xerta do not coincide with any of the ones downstream, a data extrapolation has to be undertaken. Therefore the downstream points are converted into $\log_{10}$-scale. A linear regression delivers the empirical relation $y = 1,272x - 2,3369$ with a correlation coefficient of r^2=0,9934 as can be seen in figure 5.6.

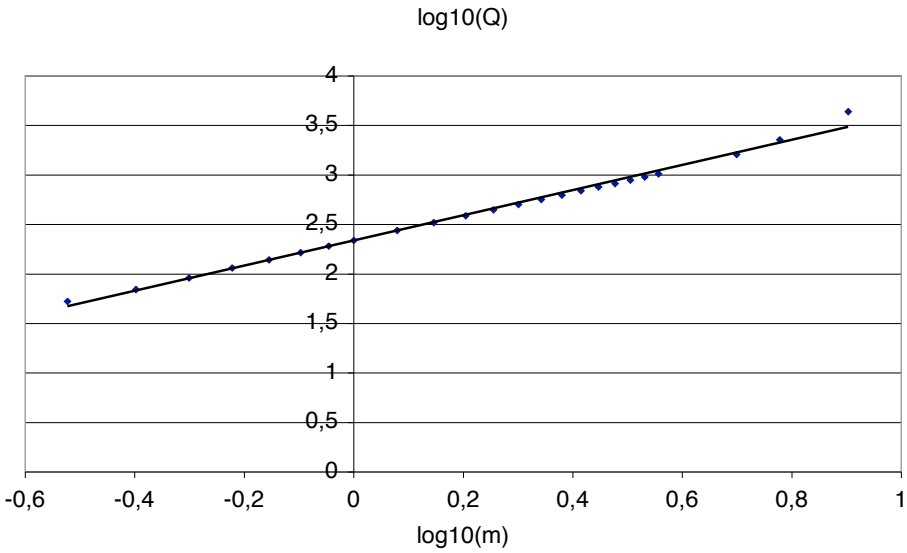

Figure 5.6: *Stage-discharge linear regression on log_{10}-scale*

Subsequently stage input values for discharges equal to upstream ones are determined as can be seen in table 5.7. Afterwards the step-backwater model can be calibrated using extrapolated downstream inputs and calibrating towards measured stages at respective discharges upstream at Xerta. In order to avoid problems due to extrapolation of extreme events, the discharge at 4380m^3/s is being omitted.

Manning n	Sim. Stage [m]	Obs. Stage [m]	Difference [m]	Error %
0,0300	7,2940	7,3000	0,0060	0,0822
0,0320	7,4550	7,3000	-0,1550	-2,1233
0,0301	7,3022	7,3000	-0,0022	-0,0301

Table 5.8: *Q=1000m^3/s Manning coefficient calibration. Simulated and Observed stage values can be found downstream of the Xerta weir.*

Initial calibration is undertaken for a discharge value of Q=1000m^3. In this calibration run the Manning coefficient is fitted along the whole reach in order to match

upstream stage values as can be seen in table 5.8. This way a Manning coefficient of n=0,0301 is being obtained.

Once the Manning coefficient is being calibrated, the model can be calibrated for other simulated discharge values. In order to do so the roughness modifier relation (see in equation 5.3.3) is being applied.

The WSL module of Phabsim disposes over a RMOD coefficient which allows for calibration due to changes in roughness with changing discharge. Thus the calibration process is being repeated for discharges mentioned, calibrating the RMOD coefficient. Doing so parameters can be obtained as seen in figure 5.7. Tabular data can be taken from table C.1.

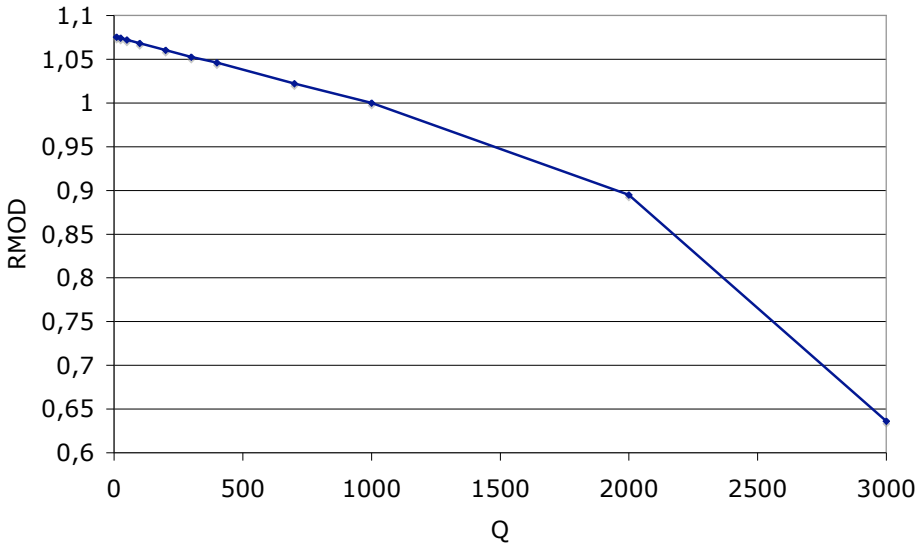

Figure 5.7: *Roughness modifier values have been calibrated between Q=400-3000 m^3/s with Manning coefficient n=0,0301. Calibrated values do not follow empirical Rmod-Q relation probably due to bank overflow. Below 400 m^3/s values are being extrapolated assuming linearity.*

The obtained values for the RMOD calibration process do not follow the theoretical distribution of the RMOD-Q relation as mentioned earlier on. This can be brought back to the fact that during most simulations bank overflow occurs with the bathymetry used. The WSL simulation model interpolates vertical ”glass-walls” as mentioned by [31]. Thus the experimental relation is being falsified, which is based on flow expansion not considering overflow. In order to extrapolate RMOD values for lower discharges to be used for the WUA modeling, it is being assumed that a linear relation in RMOD values occurs for the reach between Q=400-1000m^3/s. Applying this linear relation, the RMOD values for Q=10-300^3/s are being obtained. It shall be noted that due to a

numerical problem within the Phabsim WSL simulation modul, all calculations were undertaken elevating bathymetry data by 100m, since original bathymetry data contains negative values. Final results for calibrated water surface levels can be seen in figure 5.8.

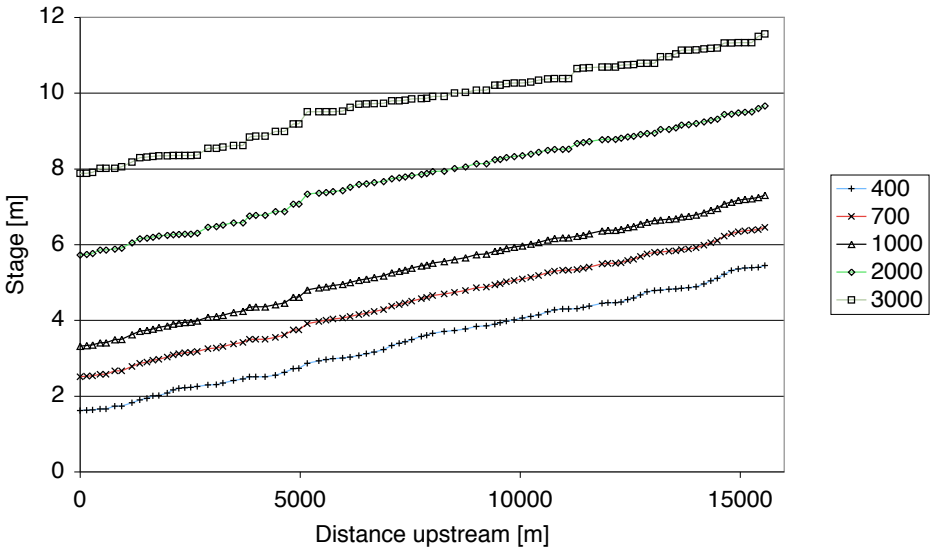

Figure 5.8: *Visualized results for water surface levels for calibrated discharges. Visualized are simulations for Q=400-3000 m^3/s. Simulations have been undertaken from Tortosa at distance zero up to downstream of the Xerta weir.*

5.3.5 Habitat Suitability Curves

Phabsim brings along a set of HSCs to be used in their laboratory sessions. Since there does not exist any HSC for the Lower Ebro concerning a locally typical species, an existent one has to be transferred. Transferability of HSCs is very much discussed topic and generally spoken wrong to be undertaken. This specific case evaluation of Phabsim though makes it necessary to dispose over a roughly applicable HSC.

Trout only survive below 21 °C temperature which apparently is exceeded at current conditions and therefore is nonexistent at this altitude. A formerly very abundant species according to de Sostoa is the Barbus graellsii (Spanish: Barbo de Graells) from the family of the Cyprinidae, called Ebrobarbe after Steindachner. This species has existed throughout the Ebro basin, though it is not as abundant any longer in the lower parts due to changes in flow regime and environment as well as overfishing in the fourties. Another species that can be found is the Squalius (Chub). For this species HSCs have been generated by [1]. HSCs used can be seen in figure 5.11, 5.10 and 5.9. Detailed

tabular data can be found in C.1, C.1 and in C.1. Since only one data point is available for the entire reach, it was decided not to consider cover/substrate curves. This was achieved by setting values to one from zero to 100, which equals a suitability index of one.

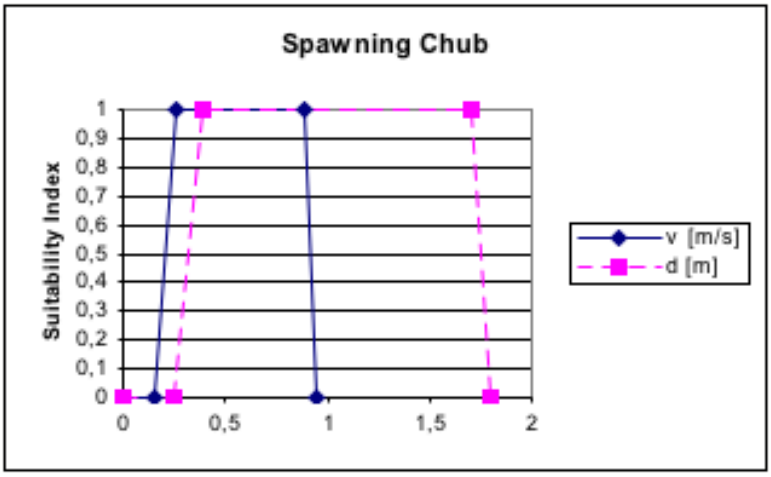

Figure 5.9: *HSC for spawning chub as seen in [1]*

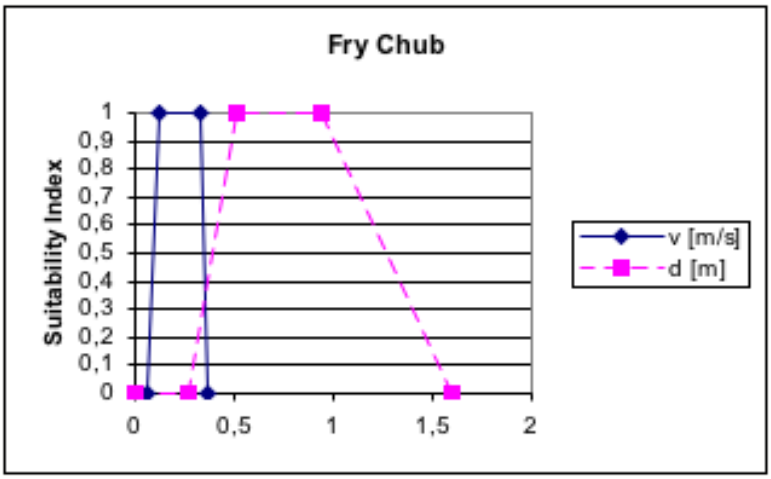

Figure 5.10: *HSC for fry chub as seen in [1]*

5.3.6 Velocities

Velocities can be calculated in several ways within Phabsim. Calculations are done by the VELSIM module. Since no velocity observations were at hand, no calibration can be undertaken and thus the most simple algorithm is used by VELSIM, based on the mass conservation equation. Cross-sectional area for each cell is defined as the 50% length to adjacent vertical sections.

5.3.7 WUA

The Weighted User Area is physically defined as plan area of the water surface over a river length (m^2/1000m), which can be interpreted directly as available habitat area per length of reach. The total usable area equals the sum of plan surface area of each of the individual cells with a river reach. Thus the larger the area available the better the reach is suited to host life. There are three methods available for calculating WUA as seen in 4.2.3 with the multiplicative, geometric and minimum. The multiplicative implies a cumulative effect (optimum when all variables are optimal), the geometric a compensatory (two optimum variable compensate for the third) and the minimum a limiting factor mechanism (habitat is not better than its worst factor).

Comparing the three available WUA methods it can be observed that the standard method and the minimum method do not differ. The geometric method generates a higher magnitude for the resulting WUA, but output is not shifted along the x-axis. This means that interpretation for recommendable flows is not altered by the WUA calculation method used for the applied HSCs. The fact that the standard and the minimum method equal in this case, might be due to that variations in substrate are not considered in this set up. This might change with higher substrate data resolution. Considered are most conservative outputs.

5.3.8 Error

In order to analyze the stability of the WUA model, it was decided to vary input values for the Phabsim simulation process by a fraction of its respective values. It was being assumed that three scenarios of error could be generated.

1. A change in discharge would resemble an error in stage-discharge observations.
2. A change in stage and Manning coefficient would resemble a change in velocity and thus an error in Manning coefficient evaluation.

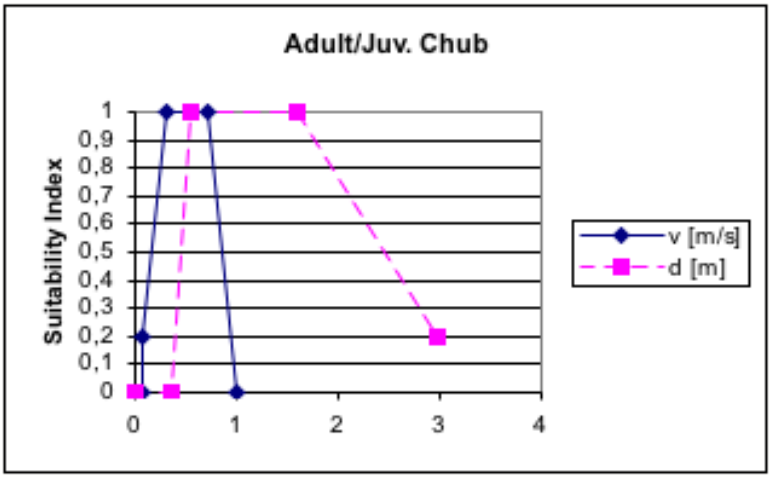

Figure 5.11: *HSC for adult/juvenile chub as seen in [1]*

3. A change in HSC values would resemble an error in estimating the habitat curves.

For scenario 1 discharge was altered by -/+10%, for scenario 2 the stage was altered by -/+10% equally and the Manning coefficient was altered by -/+15% respectively. For scenario 3, 10% of the respective discharge value were added or subtracted. Results obtained for WUA simulations with normal and altered input can be seen in figure 5.12.

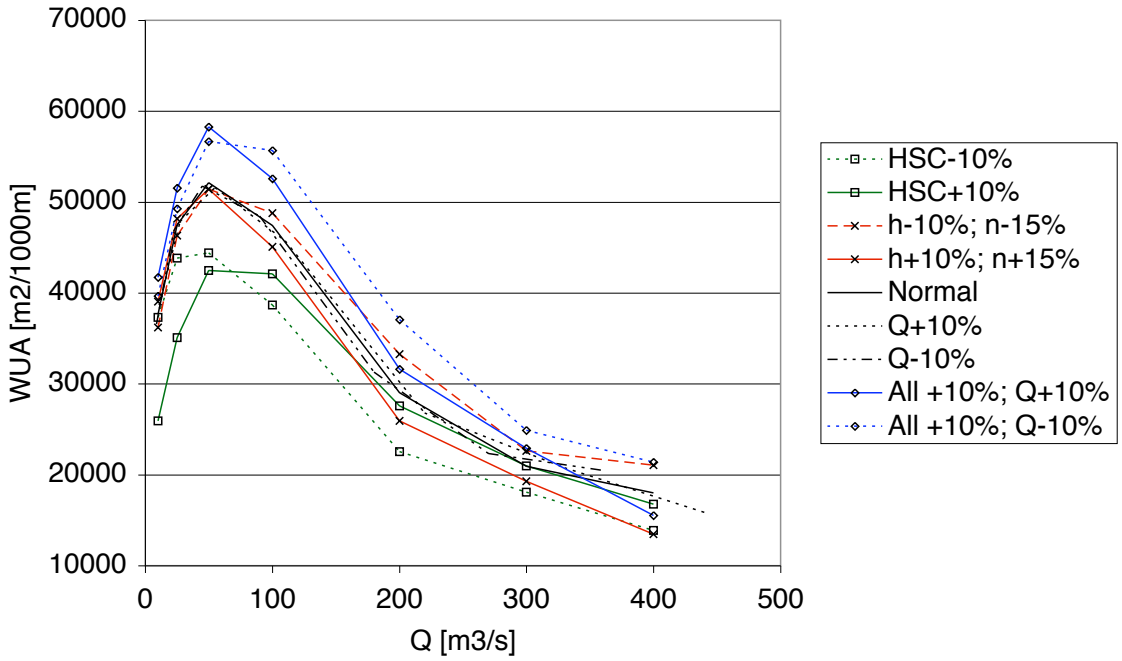

Figure 5.12: *Results of Phabsim error evaluation. Error sources are generated by shifting habitat curves along x-axis (HSC+/-10%), changing stage input and Manning coefficient (h+/-10% and n+/-15%), altering discharge input (Q+/-10%) and combining various error sources (All+10% and Q+/-%). Note that changes in HSC input cause shifts of WUA-Q relations along the x-axis, whereas other error sources only alter WUA magnitude.*

5.3.9 Results

Applying physical habitat modeling with a hydraulic 1-D backwater curve model and habitat suitability curves as mentioned earlier on can be used to calculate an optimum flow and the weighted usable area for the species in focus. Results reveal an optimum flow for the different species lifestages.

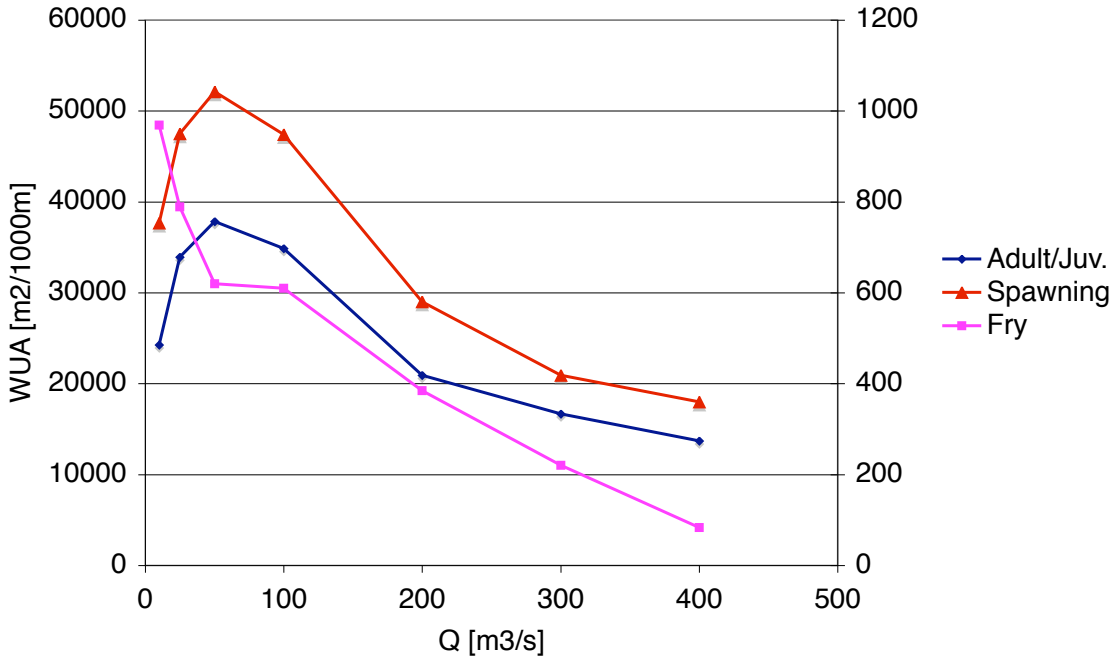

Figure 5.13: *Results of physical habitat simulation for chub. Optimum flow for adult/juvenile and spawning chub can be found around Q=50 m^3/s, whereas fry optimizes strongly for lower flows.*

Within the range of modeled discharges the optimum discharge for adult/juvenile and spawning life stages is located around Q=50 m^3/s. Higher discharge resolution at the lower end might deliver more detailed numbers. For the fry lifestage the WUA increases steeply for lower flows than Q=50 m^3/s. Flows increasing Q=100 m^3/s decrease available WUA for all life stages. Results should though be considered with care.

5.3.10 Discussion

The Phabsim model delivers optimum and minimum flows, which are physically directly related to a usable area by species considered (WUA). In this application only one habitat curve could be applied, which is not sufficient to simulate habitat variety throughout all seasons. In order to develop an optimum flow calendar more key species have to be defined throughout their lifestages with their according habitat curves.

Although WUA is calculated along the whole reach, the bathymetry should be considered, since flow velocities a.o. habitat input parameters vary strongly along cross-sections. This requires the employment of other hydraulic modeling techniques like 2-D or even 3-D in order to have more detailed information available for embankments. Thus it may well be possible to achieve WUA increase by small embankment reconstructions, e.g. for the fry lifestage which requires smaller discharges. These might be enabled by reactivating shallow embankment areas or pool-riffle architectures as well as flood plains.

5.3.11 Conclusion

Applying the Phabsim model to the reach between Xerta and Tortosa it can be concluded that

- Manning coefficient is calibrated univariatly along the whole reach with n=0,0301.
- Empiric n-Q relation does not hold due to bank overflow and RMOD values have to be extrapolated linearly for lower discharges.
- Currently only habitat curves for one species are available for application.
- WUA is an expression of physically available water surface for habitat within a river's length.
- The Phabsim model is succeptible for input error by habitat curves. Hydraulic input errors do not propagate accordingly.
- The optimum discharge for adult/juvenile and spawning chub is around Q=50 m^3/s.
- Optimum discharge for fry chub increases significantly for lower discharges than Q=50 m^3/s.
- Flows increasing Q=100 m^3/s decrease availabla WUA for all lifestages.
- Physical habitat models like the Phabsim can be combined with 2D and 3D hydraulic models likewise.